GOVERNMENT OF WESTERN AUSTRALIA

Department of **Biodiversity, Conservation and Attractions**

Biodiversity and Conservation Science

Ecophysiological performance, plant water relations and niche characteristics of *Aluta quadrata*

Annual Report 1

March 2021 – March 2022

Wolfgang Lewandrowski, Emily Tudor, Sean Tomlinson and Jason Stevens

Kings Park Science, Biodiversity and Conservation Science

Department of Biodiversity, Conservation and Attractions

Delivered April 2022 to Rio Tinto Iron Ore as part of the *Aluta quadrata* Plant Function, Habitat & Substrate Interactions Project

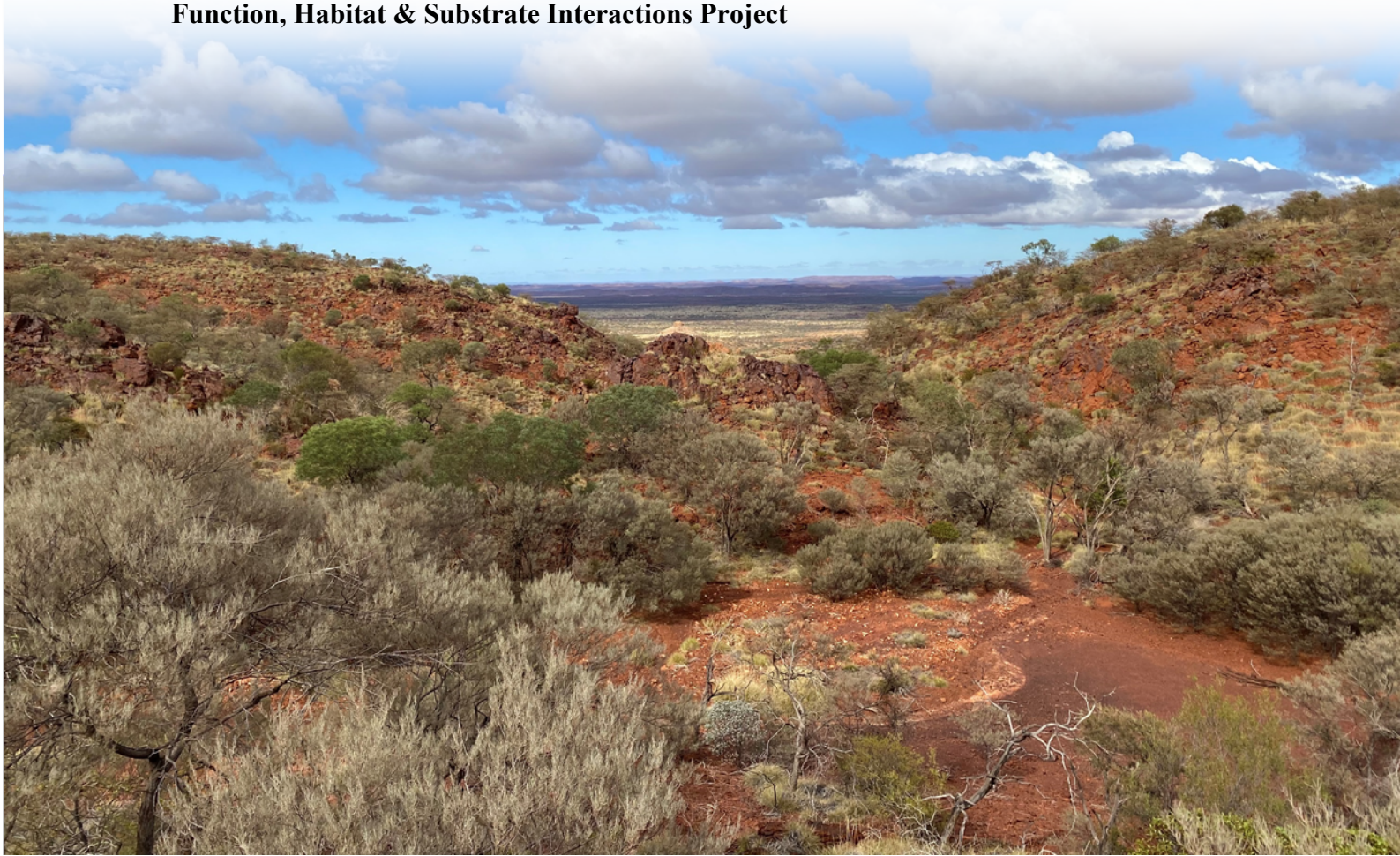

Executive summary

This annual report summarises the research conducted in Year 1 of the *Aluta quadrata* plant water use and niche characteristics. Broadly, the first year focused on: 1) completing a baseline species distribution model; 2) commencing studies on plant functioning in natural sites; and 3) collection of soil and plant samples at natural sites.

A baseline species distribution model was developed that used eight high resolution edaphic factors at approximately 25 m^2 resolution. Of these factors the model determined slope, elevation, soil bulk density and silt content strongly associated with predicted habitat suitability for *Aluta quadrata* Rye & Trudgen, with plants modelled to occur predominantly on elevated, rocky slopes, with shallow sandy soils with low silt and clay contents. Additionally, *A. quadrata* is limited in its distribution to soils with a bulk density of 1.37 – 1.43 g/cm^3. Collectively, these parameters highlight the specific edaphic niche characteristics of *A. quadrata* and provide further evidence to support this species as a slope species.

Selection of survey sites to conduct ecophysiological measurements were informed by the aforementioned habitat suitability model. Selection of survey sites was informed by the aforementioned species distribution model such that two sites were selected to represent "high-suitability habitat" and "low-suitability habitat" with *A. quadrata* present and a further two sites selected as "high-suitability habitat" and "low-suitability habitat" with *A. quadrata* absent, representing unoccupied niche.

In situ physiological performance was characterised for *A. quadrata* and a morphologically similar sympatric species, *Eremophila latrobei* F.Muell. Ecophysiological monitoring of sites identified periods of peak functioning (summer, wet) and stress (pre-summer, dry). The modelled high suitability site with *A. quadrata* present were characterised by elevated responses for gas exchange, but not always for plant available water in both species. Critical leaf water potential estimates indicated winter dry periods to be a threshold period for plant functioning, as predawn leaf water potentials rapidly decrease as seasons transition from winter to pre-summer dry periods. During these periods the majority of plants surveyed were also observed to senesce and abort flower development. Ongoing ecophysiological monitoring will further explore dynamics in plant functioning, water sourcing and niche impacts in *A. quadrata*.

Please cite this document as follows:

Lewandrowski, W., Tudor, E.P., Tomlinson, S. & Stevens, J.C. (2022) Ecophysiological performance, plant water relations and niche characteristics of *Aluta quadrata.* Annual Report 1, March 2021 - March 2022. Submitted to Rio Tinto Iron Ore, April 2022. *Aluta quadrata* Plant Function, Habitat & Substrate Interactions Project. Kings Park Science, Department of Biodiversity Conservation and Attractions.

Contacts:
Dr. Wolfgang Lewandrowski
Email: wolfgang.lewandrowski@dbca.wa.gov.au

Kings Park Science Administration
Email: scienceadmin@dbca.wa.gov.au
Kings Park Science, Department of Biodiversity Conservation and Attractions

Background

In response to a request from Rio Tinto Iron Ore (RTIO), Kings Park Science commenced research into the plant-water use and niche definition of *Aluta quadrata* Rye & Trudgen in March 2021. *A. quadrata* is a threatened myrtaceous shrub native to the Pilbara region of Western Australia which grows in three distinct populations spanning a ~38.5km distribution along the southern fringe of the Hamersley Range (Byrne et al., 2016).

Aluta quadrata grows in habitat including steep rocky slopes, steep gorges, and gullies, with a preference for southern facing slopes of rugged topography in skeletal soils, including Brockman Iron Formation substrates (Byrne et al. 2016). With the planned expansion of mining into the Western Range area (pending approval) there will likely be impacts on the Western Range population.

Defining the plant water-use attributes of the species and its substrate interactions will enable a greater understanding of the niche that this plant occupies. Here we focus on the physical structure, hydrology and chemistry of habitat substrates, surrounding micro-climates, and the physiological response of *A. quadrata* to variation in these parameters.

The broad research objectives of this program are to:

1. Define the plant water-use attributes and substrate interactions of *A. quadrata*
2. Examine the physiological responses of *A. quadrata* in relation to the topography, hydrology, and soil chemistry of habitats
3. Characterise the niche that *A. quadrata* occupies and establish meaningful biological correlates between habitat suitability and plant performance

Key performance indicators

To achieve the broad objectives, the research program is focused on developing a high-resolution species distribution model for *A. quadrata* that is informed by edaphic factors and climate associated correlates. Ecophysiological surveys on plant functioning and plant-soil interactions will test and ground-truth initial modelling and provide a baseline for subsequent model refinement. This current report focusses on delivering key performance indicators #1 and #3 (Table 1). With the exception of KPI #5, all of the agreed KPI's have been completed. The completion of KPI#5 is expected for June 2022, with results to be reported in Annual Report 2.

Table 1. Key performance indicators delivered in the first research year by Kings Park Science.

KPI #	Description	Period	Status
1	Baseline Species Distribution modelling completed	Current	KPI Met
3	Ecophysiological studies commenced	Current	KPI Met
5	Analysis of soil samples at natural sites completed	Current	In Progress

KP1 – Baseline species distribution modelling

Recent advances in species distribution modelling enable species distribution projections constructed based on physical soil characteristics and geomorphology at approximately 25 m^2 resolution (Tomlinson et al. 2020). Broadly following the methodology outlined in Tomlinson et al. (2020) we constructed a species distribution model for *A. quadrata* using presence point data and publicly available datasets describing the physical soil characteristics and geomorphology. High-resolution spatial data for aspect, elevation and slope were sourced from Gallant and Austin (2012a), and Gallant and Austin (2012b), while spatial data describing the percentage of clay, silt and sand at 15cm depth

were sourced from Viscarra Rossel et al. (2014a), Viscarra Rossel et al. (2014b) and Viscarra Rossel et al. (2014c). These data were all aligned, and where necessary downscaled by bilinear scaling using the elevation data as a template using the 'raster' package in the R statistical environment (R Core Team, 2021). Soil bulk density (Mg/m^3) and depth were interpolated for each 25 m^2 grid location from national soil data sourced from the Australian Collaborative Land Evaluation Program (ACLEP; www.clw.csiro.au/aclep).

We used the maximum entropy algorithm implemented in MaxEnt version 3.3.3a (Phillips et al. 2006, Phillips and Dudík 2008) to model the local distribution of *A. quadrata* within the three known populations along the southern edge of the Hamersley Range. Default MaxEnt parameter settings were used to develop logistic likelihoods of occurrence, with a value of 1 representing the highest likelihood (Phillips 2008). To remove presence outliers, we applied a 10^{th} percentile training presence which excludes observations considered to be the 10% extreme observations. This was done to represent the "core" of the known distribution and minimise the impact of uncharacteristic presence data.

Pilot models were developed using all the available candidate layers (elevation, aspect, slope, clay, sand and silt content, and bulk density) and were further refined by removing layers that contributed less than 5% contribution to fit (Table 2). The edaphic factors that the MaxEnt algorithm determined to be the best predictors of the probability of occurrence of *A. quadrata* were slope (%), elevation (m), soil bulk density (g/cm^3) and silt content (%). As such, the final model was refined to these variables (Figure 1; Appendix 1). The spatial projection was defined to encompass three IBRA bioregions—the Pilbara (PIL), Little Sandy Desert (LSD) and Gascoyne (GAS).

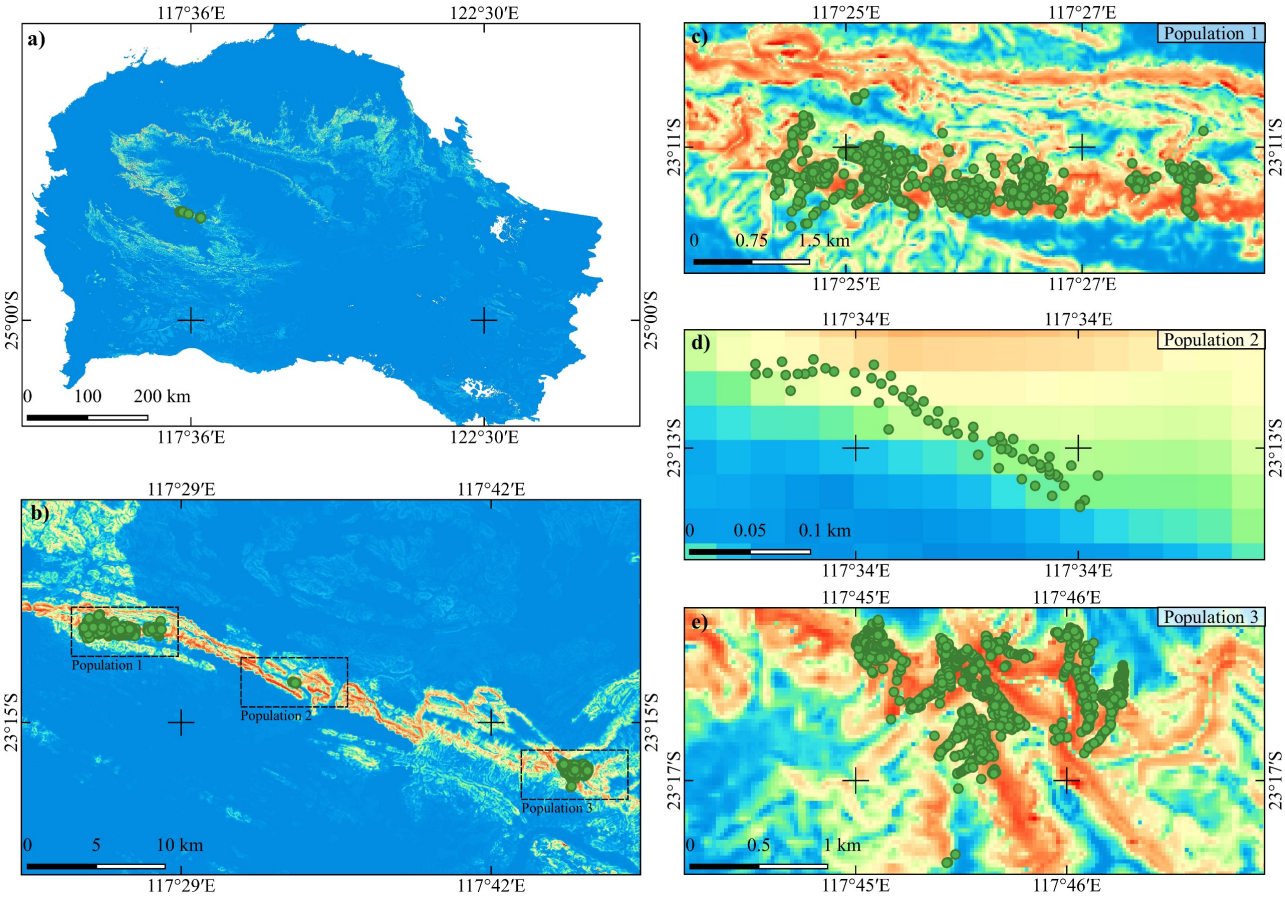

Figure 1: Projected species distribution and likelihood of occurrence for Aluta quadrata derived from a MaxEnt model. a) Full spatial projection was defined to encompass three IBRA bioregions—the Pilbara (PIL), Little Sandy Desert (LSD) and Gascoyne (GAS); b) Extent of occurrence for known presences of *A. quadrata* defined by three distinct populations; c) Western Ranges population ; d) Pirraburdoo population; c) Howie's Hole population. Increasing intensity of colour (from blue to red) indicates a higher likelihood of occurrence. High resolution maps for figure 1a and 1b correspond to Appendix 1 and 2, respectively.

Following the broad methodology and justification outlined in (Tomlinson et al. 2020) we interpolated a climate model to estimate atmospheric and edaphic conditions associated with the spatial projection of the MaxEnt distribution model. Essentially, microclimatic projections for summer (wet) and winter (dry) ambient air temperature, surface soil temperatures, soil water potential at 20 cm depth and solar radiance were calculated and averaged using the "micro-global" algorithm of the NicheMapR statistical package (Kearney 2016) in R (R Core Team, 2021).

To minimise the computational load of calculating microclimatic models at every location across the study area, we downscaled our spatial data to 20 arc-second resolution (approximately 300 km^2), resulting in 1651622 grid point locations. At each point location, representing the centroid of the associated grid square, the physical soil characteristics were summarised into a format appropriate for NicheMapR following a freely available soil texture calculator produced by the United States Department of Agriculture (Soil Texture Calculator | NRCS Soils (usda.gov)) adapted to a computer algorithm similar to Gerakis and Baer (1999). For each point location we calculated hourly microclimatic conditions for every day of the year, using five replicate years' resampling form the interpolated climate model. Hourly values were then summarised by average daily conditions. For lack of any quantified proxies for vegetation shading, all microclimatic projections were run assuming full

sun, with full recognition that this does not capture all the microclimatic variation across the course of the day.

We identified the consecutive 90-day period when air temperature was warmest, when air temperature was coldest, and also the highest and lowest rainfall respectively. At each location hourly values were summarised as daily averages for these 90 days were again summarised to a mean wettest and driest quarter average for each point location over a 10-year period. In order to rescale these data back to the native one arc-second resolution, we used an interpolation approach (Carter et al. 2018), where the microclimatic data at our 20 arc-sec resolution were fed into a generalised linear model (GLM) informed by the edaphic and geomorphological data for each location. We generated unique GLMs for each microclimatic parameter for the wettest and driest quarters. We then used these GLMs to estimate the same parameters at point locations describing the grid centroids of the one arc-sec landscape using the "predict" function in R.

We extracted the climate data for 1000 random points within the training extent of the MaxEnt distribution model to construct a linear model describing the microclimatic correlates of the modelled likelihood of occurrence and habitat suitability. Following the construction of a 'full' model we applied a model reduction using the *dredge* function within the '*MuMIn'* package (Bartoń 2014), and the models were examined by Akaike's Information Criterion for small sample sizes (AICc; Burnham and Anderson 2002). However, model reductions did not substantially increase model parsimony and the full model was retained and reported (Table 3).

Table 2. Relative contributions of topographic and edaphic variables contributing to the *Aluta quadrata* MaxEnt species distribution model. Refer to Appendix 4−7 for spatial representations of the top four contributing microclimatic factors. Refer to Appendix 8 for summary statistics (mean ± se) for each variable as it pertains to a categorical representation of the projected habitat suitability.

Variable	Contribution to Model (%)	Permutation Importance
Slope (%)	56.2	10.8
Elevation (m)	13.1	43.5
Soil Bulk Density (g/cm^3)	12.4	31.5
Silt Content (%)	10.6	6.9
Aspect (°)	4.4	2.0
Sand Content (%)	2.0	3.7
Clay Content (%)	1.1	1.0
Soil Depth (m)	0.2	0.6

Results:

The final species distribution model of *A. quadrata* resulted in a high area under the curve (AUC = 0.935). A model reflecting an AUC greater than 0.7 is considered to be a plausible and likely representation of the probability of occurrence for a given species (Pearce & Ferrier, 2000). The average habitat suitability index (HSI) at known occurrence locations was 0.68 (range = 0.02 to 0.92). Over 60% of the known locations (~27700 individual plants) were modelled to persist in habitat exceeding a HSI of 0.7. Only 5039 individuals were modeled to persist in habitat with a HSI <0.5. The strongest contributor to the modelled distribution was slope (56.2%;) followed by elevation (13.1%) and bulk density (12.4%). As such, *A. quadrata* was modelled to occur predominantly on elevated, rocky slopes along the Hamersley Ranges. The northern fringes of the Hammersley Ranges were also predicted to have a high likelihood of occurrence, despite no known populations existing beyond the three populations identified along the southern extent of the range. Additionally, the intervening area between

the three extant populations is predicted to have a high likelihood (up to 98.2%) of supporting *A. quadrata.*

We constructed linear models to understand climatic correlates of the modelled likelihood of occurrence and habitat suitability (Table 3). Microclimatic factors were found to have a significant association with the likelihood of occurrence of *A. quadrata* (Adjusted R^2 = 0.31, $F_{8,991}$ = 56.37, P <0.001). Model dredging highlighted that the full linear model (AICc = -1898.2, Log-likelihood = 959.232) indicated a positive relationship between the likelihood of occurrence of *A. quadrata* and microclimatic factors is driven most strongly by annual soil water potential (Summer Wet: $F_{1,991}$ = 135.03, P <0.001; Winter Dry: $F_{1,991}$ = 103.37, P <0.001; Table 3), followed by winter temperatures ($F_{1,991}$ = 75.96, P <0.001; Table 3), summer solar radiation ($F_{1,991}$ = 21.08, P <0.001; Table 3) and summer soil temperatures ($F_{1,991}$ = 16.72, P <0.001; Table 3).

Table 3. Summary statistics of microclimatic conditions calculated at 1000 random point samples across the projected landscape and output of one-way analysis of variation examining the microclimatic correlates of the likelihood of occurrence for *Aluta quadrata.* Refer to Appendix 9 for summary plots of these data.

Season	Factor	$F_{(1,991)}$	Pr (>F)
Summer Wet	Solar Radiance (Lumens)	0.968	0.325
	Ambient Temperature (°C)	75.963	**<0.001**
	Soil Temperature (°C)	0.782	0.377
	Soil Water Potential (kPa)	103.366	**<0.001**
Winter Dry	Solar Radiance (Lumens)	21.079	**<0.001**
	Ambient Temperature (°C)	0.034	0.854
	Soil Temperature (°C)	16.729	**<0.001**
	Soil Water Potential (kPa)	135.026	**<0.001**

Interpretation of microclimate associations: *A. quadrata* was modelled to be restricted to comparatively wetter soils in an otherwise arid environment potentially indicating that the current distribution of *A. quadrata* is refugial and limited to localized wetter and milder conditions compared to the surrounding landscape. This is consistent with models describing the realized niche of other shallow-soil endemic species in arid habitats of Western Australia (Tomlinson et al 2020; Tomlinson unpublished), and rocky habitats appear to offer locally moist microhabitats that may be refugia in otherwise hostile habitat for these species. The identification of vacant areas of suitable habitat is also a common outcome in studies of habitat suitability of short-range endemic flora and is usually attributed to either stochastic extirpation of any populations that once occupied the area, or a failure to colonize the habitat due to poor dispersal ability (Fiedler & Ahouse, 1992; Hopper & Gioia, 2004).

Microclimatic associations within the study system appear to be driven primarily by soil water potentials (kPa) across both the wet and dry seasons. This would suggest that the soils retain water at the locations where *A. quadrata* occurs. These trends represent preliminary analysis into the climatic drivers of *A. quadrata* occurrence and physiological performance. Ongoing work will aim to delineate these relationships further. However, it is important to note that these microclimatic factors do not contribute to the projection of habitat suitability that was founded on the basis of edaphic factors. Instead, these data represent correlative associations between the aforementioned habitat suitability estimate.

KPI 3 – Studies of plant functioning in natural sites

Site Selection

In situ physiological performance was characterised for *A. quadrata* and a morphologically similar sympatric species, *Eremophila latrobei*. Physiological measurements were conducted across four sites over three monitoring periods (22nd-29th August 2021, 24th-31st October 2021, and 13th-19th March 2022). Selection of these survey sites was informed by the aforementioned habitat suitability model such that two sites were selected to represent "high-suitability habitat" and "low-suitability habitat" with *A. quadrata* present and a further two sites selected as "high-suitability habitat" and "low-suitability habitat" with *A. quadrata* absent, representing unoccupied niche (Table 4). Here, we only present preliminary results from 'High Suitability Occupied' and 'Low Suitability Occupied' to demonstrate the trends in plant performance to-date. All data relating to the Unoccupied sites will be presented following the completion of a dataset representing a full annual cycle (i.e., four monitoring periods).

Table 4: Location and site classification of high and low suitability sites that were selected for ecophysiological monitoring of *Aluta quadrata* and *Eremophila latrobei* in the Western Ranges, Pilbara. Average habitat suitability index (HSI) was calculated from the projected MaxEnt Distribution and N represents the number of plants sampled in each location.

Site	Location (Lat, Long)	Classification	Avg. HSI	N
S1	-23.180062, 117.423802	High Suitability Occupied	74.5	20
S2	-23.177255, 117.420814	High Suitability Unoccupied	79.0	10
S3	-23.180829, 117.427142	Low Suitability Occupied	21.4	20
S4	-23.179032, 117.429558	Low Suitability Unoccupied	28.6	10

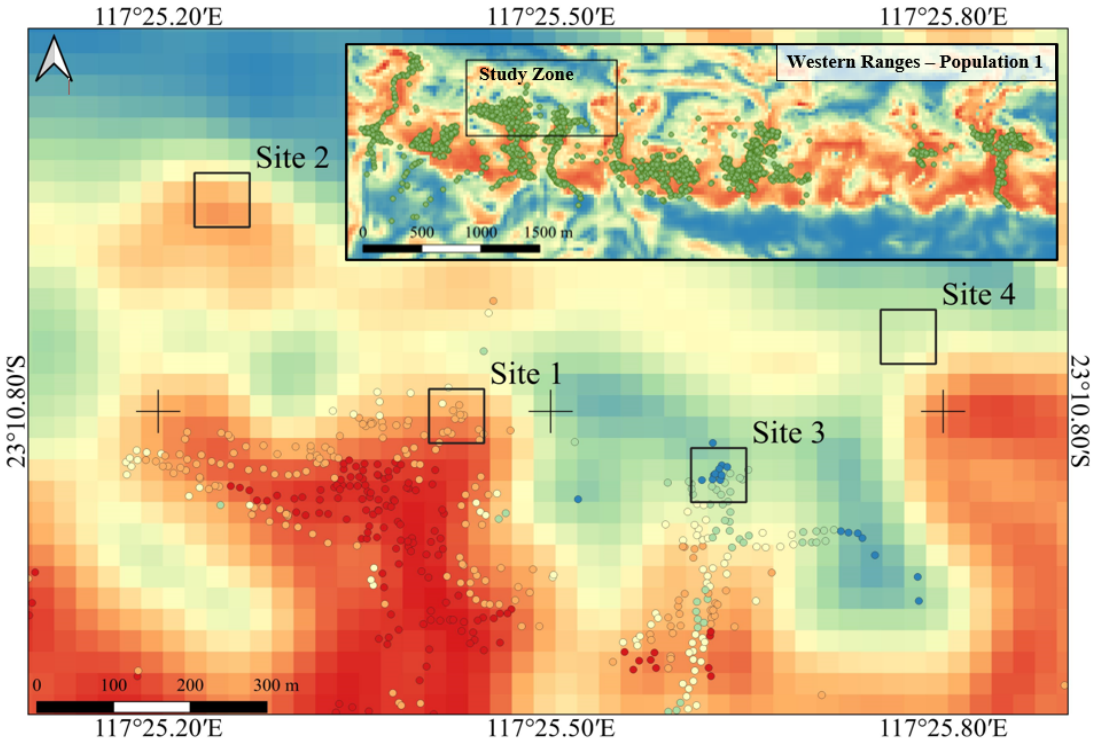

Figure 2: Map of the niche-model indicating the locations of the four study sites within the study zone. Results for plant functioning are presented for Sites 1 and 3 in this present report. High resolution map of Figure 2 corresponds to Appendix 3.

Ecophysiological assessments quantified in high and low suitability sites

Ecophysiological evaluation of plant responses to environmental conditions and stressors can provide mechanistic insights into plant performance across sites that have different habitat/niche characteristics (Tomlinson et al. 2021, Valliere et al. 2021). We undertook a suite of measurements (see Table 5) that provided an insight into growth and productivity (photosynthetic rate), plant-water use (stomatal conductance and transpiration rate), plant-water stress (pre-dawn and mid-day leaf water potential), and plant health (chlorophyll fluorescence indicator for maximum quantum yield - F_v/F_m).

Table 5. Selected physiological plant traits and the implications for plant performance presented in this annual report [adapted from Valliere et al. (2021)].

Trait	Implication of comparative measurement
Photosynthetic rate (A)	High photosynthetic rates may indicate favorable site/environmental conditions or that a given species is suitable for the site. Higher photosynthetic rates are also associated with higher growth rates in plants.
Transpiration (E)	High rates of transpiration may indicate favorable plant water status.
Stomatal conductance (g_s)	A measure of the degree of stomatal opening which can be used as an indicator of plant water status. Increased stomatal conductance leads to increases in photosynthetic and transpiration rates.
Plant health measured via chlorophyll fluorescence: maximum quantum yield (F_v/F_m)	Provides a measure of photosynthetic and chlorophyll performance and can be used to assess levels of plant stress (e.g., photoinhibition due to high light). F_v/F_m ratios change gradually in response to environmental stresses and are less sensitive to immediate stress in contrast to A, E and g_s. Typical values for healthy plants are 0.8 – 0.85. For many wild species in the arid zone, healthy plants are more commonly 0.7-0.8. Stress plants are characteristically <0.6, though these responses must be complimented by other physiological and morphological measures.
Pre-dawn leaf water potential (Ψ_{pd})	Provides an indication of soil water availability, where lower Ψ_{pd} indicates increasing water deficit. This measure typically is quantified prior to first light, when plants equilibrate to the soil water status due to stomatal closure.
Mid-day leaf water potential (Ψ_{md})	Useful for assessing drought strategies across species; drought avoiders will maintain a constant Ψ_{md} while drought tolerators will exhibit a drop in Ψ_{md}. Mid-day leaf water potentials are measured at the peak stress time of day.

Gas exchange measurements: Photosynthetic rate, stomatal conductance and transpiration rate

For each of the species, photosynthetic rate (A), stomatal conductance (g_s), and transpiration rate (E) were measured using a LI-6400XT portable photosynthesis system and gas exchange analyser (LI-COR Biosciences, Lincoln, NE, USA) that was equipped with a 6400-40 leaf chamber fluorometer. All measurements were taken between 08:00−12:00 pm, representing the time where the plant is most photosynthetically active prior to stomatal closure. All measurements were quantified under constant light saturated conditions, whereby photosynthetic active radiation was maintained at 1200 µmol m^{-2} s^{-1}. Additionally, internal carbon dioxide concentrations were equilibrated to 400 µmol CO_2 mol^{-1} and relative humidity was maintained between 50-70%. Thermal conditions were ambient throughout all measurements to reflect seasonal temperature conditions at the time of measurement. All measurements were quantified on up to 10 replicate plants. On each plant, three replicate measurements were quantified on 2-3 individual tufts comprised of mature needle-like leaves that were located on the terminal stem. For each of the measurements, leaf-tufts were allowed to equilibrate to the internal leaf chamber conditions, whereby the stability of gas exchange parameters was monitored in real-time. Following measurement, leaf-tufts that were measured within the chamber were harvested from the plant and returned to the ecophysiology laboratory for leaf area analysis. All measurements were leaf-area corrected prior to statistical analysis.

Leaf water potential

Leaf water potential measurements were conducted in order to determine plant available water (predawn measurements) and plant water status at the time of stomatal closure (mid-day measurements) (Turner 1981). Predawn (Ψ_{pd}) sampling occurred prior to first light (between 0300-0400 am), whereby terminal stems that were approximately 10 cm in length were harvested from plants and stored within a sealed foil bag in cool conditions, prior to leaf water potential assessment. Mid-day (Ψ_{md}) sampling occurred approximately between 1045-1100 am during summer and between 1100-1200 pm in winter, representing the conditions of peak stress and approximate solar noon for the region. All measurements were conducted within 15-30 minutes of harvesting, whereby terminal stems were cut at a 45° angle and immediately secured within a Scholander Pressure Chamber (Model 1000, PMS Instruments Co, USA) with the cut stem externally exposed prior to pressurisation (<100 bar). For each species 10 replicate plants were measured, whereby 2-3 measurements were quantified per plant for Ψ_{pd} measurements, and a single replicate measurement quantified per plant for Ψ_{md} measurements.

Chlorophyll fluorescence: maximum quantum yield

Prior to Ψ_{pd} assessment, chlorophyll fluorescence measurements relating to maximum quantum yield (F_v/F_m) were quantified using a chlorophyll fluorometer (PocketPI, Hansatech Instruments Ltd, UK) on leaf-tufts for each replicate terminal stem, resulting in 2-3 replicate measurements across 10 plants for each species, per site. Dark adaptation was not required for leaf-tufts, as stems were harvested in the dark during the predawn measurement window.

Statistical analysis – preliminary

All ecophysiological parameters (A, g_s, E, F_v/F_m, Ψ_{pd}, Ψ_{md}) were analysed by fitting linear mixed effects models, using 'lmer'-function from the lme4-package (Bates 2010, Bates et al. 2015) in the statistical environment, R (R Core Team 2021). For each model, we fixed the monitoring period (August, 2021; October, 2021; and March 2022), species (*A.quadrata*; and *E.latrobei*) and site suitability (high; and low) as main effects and inspected model performance by ranking models based on the AIC-index, conditional and marginal R^2-values (Nakagawa and Schielzeth 2013), by comparing additive (monitoring period + species + site suitability) versus interaction models (monitoring period x species

x site suitability). Replicate measurements on leaves of plants were considered random effects for species nested within the monitoring period). As both additive and interaction models provided similar conditional and marginal R^2-values > 0.66, the results for the simpler additive model are presented in this report. After fitting models, graphical analysis of residuals assessed the homogeneity of the model variance, linearity, collinearity, and log-transformation of the response-data occurred as necessary.

Further analysis was conducted to identify critical leaf water potential (Ψ_{crit}), describing a threshold leaf Ψ, below which plant water-use rapid decreases and a trait for characterising drought-stress. To determine Ψ_{crit}, the difference between Ψ_{md} and Ψ_{pd} was calculated and regressed against Ψ_{pd}-measurements using second order-polynomial regressions. The Ψ_{crit} threshold was interpolated from the peak-response in the second order-polynomial regression curve.

Results:

Ecophysiological monitoring identified peak (i.e., elevated plant functioning; see March, 2022; Figure 3) and stress periods (i.e., lowest plant functioning; see October, 2021; Figure 3) for plant functioning in species across both high and low suitability sites. Pre-summer dry conditions (see October, 2021; Figure 3) represented at least 90% in reductions across gas exchange ($A_{\text{Mon.period}}$: $F_{2,145} = 3.14$, $P = 0.04$; $E_{\text{Mon.period}}$: 2,188, $P = 0.0189$; Table 6) maximum quantum yield (Fv/ $Fm_{\text{Mon.period}}$: $F_{2,280} = 9.83$, $P < 0.001$, Table 6) and leaf water potentials ($\Psi_{pd\ \text{Mon.period}}$: $F_{2,275}$=21.8822, $P < 0.001$; $\Psi_{md\ \text{Mon.period}}$: $F_{1,131}$=5.3201, P <0.01; Table 6) in both high and low suitability sites.

There were consistent site differences measured for gas exchange for A ($F_{1,145}$=10.2, $P < 0.001$; Table 6), gs ($F_{1,188}$=5.1368, $P = 0.0248$; Table 6) and E ($F_{1,188}$=7.7830, $P < 0.01$; Table 6), with elevated measurements of 6-25% in *A.quadrata* and 17-41% in *E. latrobei* quantified in high suitability sites compared to low suitability sites (Figure 3). The largest differences for gas exchange measurements between sites were consistently measured during the summer wet (see March, 2022; Figure 3). Maximum quantum yield measures varied weakly between high and low suitability sites (Fv/ Fm_{Site}: $F_{1,280}$=0.33, $P = 0.566$; Table 6; Figure 3), and were more strongly influenced by species differences (Fv/Fm_{Species}: $F_{1,280} = 39.57$, $P < 0.001$; Table 6) and the monitoring period (Fv/ $Fm_{\text{Mon.period}}$: $F_{2,280} = 9.83$, $P < 0.001$; Table 6). Species were generally dissimilar across most measurements(Figure 3), with *E. latrobei* presenting elevated responses compared to *A. quadrata* plants for gas exchange (A_{Species}: $F_{1,145}$=25.05, gs_{Species}: $F_{1,145} = 7.63$, E_{Species}: $F_{1,145} = 11.79$; all $P < 0.001$; Table 6); and maximum quantum yield measurements ($F_v/F_{m\text{Species}}$: $F_{1,280}$=39.57, $P < 0.001$; Table 6) , but not for leaf water potentials ($\Psi_{pd\ \text{Species}}$: $F_{2,275}$=3.44, $P = 0.065$; $\Psi_{md\ \text{Species}}$: $F_{1,131}$=0.51, $P = 0.476$; Table 6).

Particularly during the pre-summer dry (October, 2021; Figure 3), maximum quantum yield measures for F_v/F_m were on average <0.3 in *A. quadrata* and > 0.4 in *E. latrobei.* Field observations further support this period to coincide with plant senescence in both species (data not shown). The low F_v/F_m measures infer that plants are experiencing increases in stress, which are further corroborated by very low Ψ_{pd} and Ψ_{md} between -8 MPa and -10 MPa that indicative of high soil water deficits (Figure 3). In contrast, Ψ_{pd} and Ψ_{md} were up to five-fold higher during peak functioning periods for gas exchange measurements (see March 2022; Figure 3). Ψ_{crit} were estimated at -3.79 MPa and -4.52 MPa for *A. quadrata* and *E. latrobei,* respectively (see Figure 4). These estimates roughly coincide with measurements undertaken during the winter dry season for both species (see August, 2021; Figure 3). These estimates also coincide with decreased gas exchange and an overall reduction in maximum quantum yield (i.e., decreases in plant health) as seasons transition into the peak stress period (October, 2021; Figure 3).

Interpretations of the preliminary trends: Ecophysiological monitoring identified peak (i.e., elevated plant functioning; see March, 2022) and stress periods (i.e., lowest plant functioning; see October, 2021) for plant functioning in species across both high and low suitability sites (Figure 3). While not reported, these periods coincide with peak plant growth and senescence in both species. While *E. latrobei* plants were slightly more responsive than *A. quadrata* across the gas exchange measurements, the lower F_v/F_m

ratios in *A. quadrata* could indicate a decrease in plant health, though no mortality of the surveyed plants has been observed to-date. Elevated gas exchange measures for *A,* g_s and *E* indicated increased ecophysiological functioning for the high suitability site in contrast to the low suitability site and are likely driven by complex interactions between plants and the edaphic/ climate factors to be explored in future research. These include i) plant leaf tissue and soil chemical/physical analyses to understand differences in mineral nutrition, and differences in the factors that were identified as important drivers in the baseline model between sites; ii) variation in environmental factors such as water availability, temperature, and solar radiation on plant individuals between sites; and iii) understanding water-sourcing in *A. quadrata* during wet and dry seasons. Further analysis will also evaluate physiological patterns in *E. latrobei* in sites where *A. quadrata* are absent to verify if suitability patterns exist.

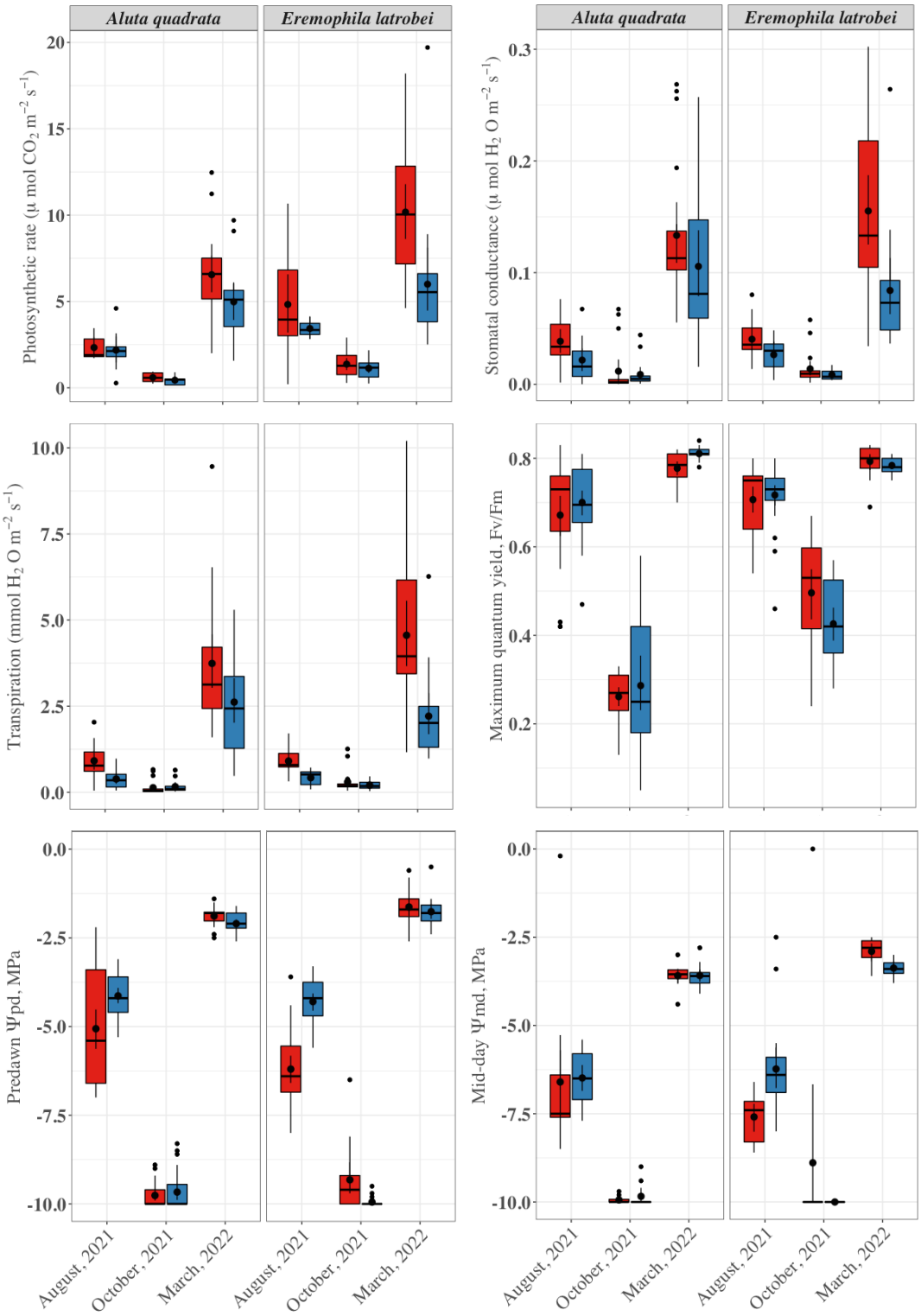

Figure 3: Ecophysiological parameters (Photosynthetic rate - *A*, stomatal conductance - g_s, transpiration rate - *E*, maximum quantum yield - F_v/F_m, predawn Ψ_{pd} and mid-day Ψ_{md}) monitored in August, October 2021 and March 2022, representing winter dry, pre-summer dry, and summer wet conditions in high (red) and low (blue) suitability sites where *Aluta quadrata* plants are present. All parameters are plotted as box and whisker plots, indicating minimum, 25th, median, 75th percentiles, maximum, and outliers in the data. Point-estimates within the box and whisker plot are means with 95% confidence intervals.

Table 6. Summary statistics of factors Species (*Aluta quadrata;* and *Eremophila latrobei*), Site (High; and Low suitability), and Monitoring period (August, 2021; October, 2021; and March, 2022) from linear mixed effects models for ecophysiological responses.

	Response	Factor	DF, Df.res	F	Pr(>F)
Gas exchange measures	Photosynthetic rate (A)	Site	1, 114	10.20	**<0.001**
		Species	1, 118	25.0492	**<0.001**
		Mon. period	2, 147148	3.14	**0.043**
	Stomatal conductance (g_s)	Site	1, 152	5.1368	**0.0248**
		Species	1, 158	7.6251	**<0.01**
		Mon. period	2, 299940	2.04	0.30
	Transpiration (E)	Site	1, 150	7.7830	**<0.01**
		Species	1, 158	11.7858	**<0.001**
		Mon. period	2, 299940	3.9638	**0.0189**
Plant health	Maximum quantum yield (F_v/F_m)	Site	1, 221	0.33	0.566
		Species	1, 239	39.5653	**<0.001**
		Mon. period	2, 163041	9.83	**<0.001**
Pant water stress	Predawn leaf water potential, (Ψ_{pd})	Site	1, 216	18.8969	**<0.001**
		Species	1, 235	3.4355	0.065
		Mon. period	2, 323405	21.8822	**<0.001**
	Mid-day leaf water potential, (Ψ_{md})	Site	1, 114	0.1622	0.687
		Species	1, 118	0.5097	0.476
		Mon. period	1, 91772	5.3201	**<0.01**

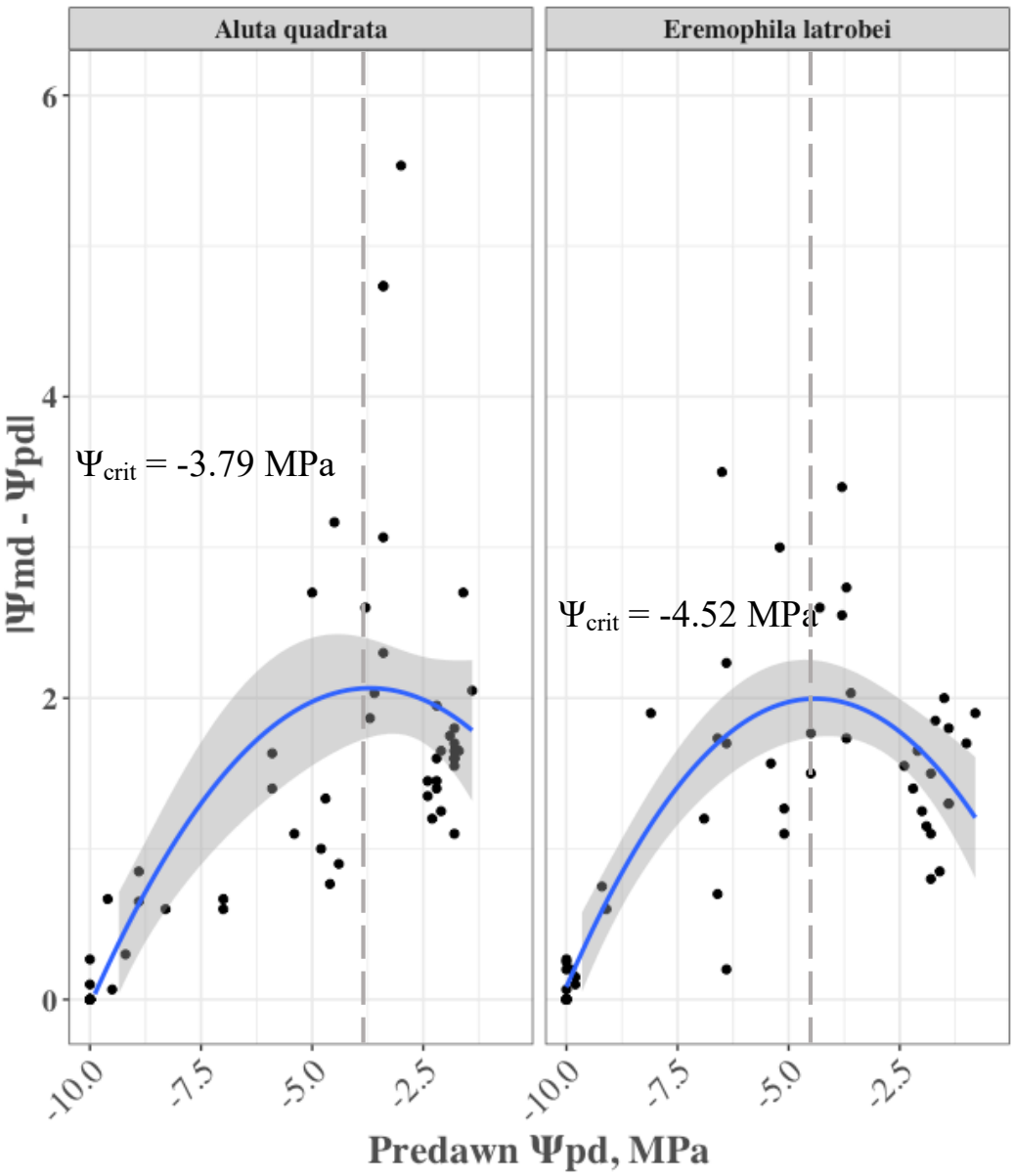

Figure 4: Ψ_{crit} estimation in *Aluta quadrata* and *E. latrobei*. Ψ_{crit} is a threshold describing responses to drought. Decreases from the Ψ_{crit} in more negative Ψ_{pd} are indicative of lower plant-water use as a consequence of drought-stress.

KPI 5 – Analysis of soil samples at natural sites.

In the sites where the ecophysiological surveys are currently undertaken, plant leaf tissue and soil samples were collected in August, 2021 and March, 2022 on ten *A.quadrata* and ten *E. latrobei* and their approximate surrounding soil environment, equating to 60 plant tissue samples and 40 soil samples. The total sample weight was approximately less than 5-10 g per plant and up to 250 ml for soils. All samples are currently in the process of analysis to determine mineral nutrition and soil physicochemical variation between high and low suitability sites. The analysis will be reported in the next annual report.

Key performance indicators to be addressed in Year 2

Year 2 research will focus on the refinement of the baseline species distribution modelling. These model refinements will be informed by the ecophysiological patterns, differences in soil chemical and physical features associated with the edaphic correlates that were determined as significant in the baseline model and interrogation of climate associated drivers, such as temperature and soil moisture.

Ecophysiological monitoring will be refined after a complete annual cycle is collected. It is anticipated that additional sites may be considered to test and validate niche suitability impacts on plant performance.

Understanding plant water-sourcing dynamics is critical for determining if *A. quadrata* plants are sourcing water from the groundwater table or from the atmosphere. These dynamics may vary strongly between seasons (wet vs dry), and along the ridge. As such, isotopic studies will be conducted along a downward slope gradient on *A. quadrata* to determine variation in water sourcing requirements during summer wet, and winter dry periods.

Table 7. Key performance indicators planned for delivery in the second research year by Kings Park Science.

KPI	KPI Description	Period	Status
2	Refined Species Distribution modelling completed	Year 1 → 3	Commenced
3	Ecophysiological studies – ongoing	Year 1 → 3	Commenced
5	Analysis of soil samples at natural sites completed	Year 1 → 2	Commenced
6	Isotopic studies of plant water sourcing in natural sites commenced	Year 2	Commencing April
7	Isotopic studies of plant water sourcing in natural sites completed	Year 2	*Due December

*anticipated completion, pending sampling and external analysis

Acknowledgement

We acknowledge the traditional custodians of the land on which this research is taking place and pay our deepest respects to elders past, present and emerging. We also would like to thank Rio Tinto Iron Tinto for providing project support, and acknowledge Hayden Ajduk (RTIO), Greg Cawthray (School of Biological Science, The University of Western Australia) and Rebecca Campbell (Kings Park Science) for discussions, logistics and support throughout the research year.

References

Bartoń, K. 2014. Package 'MuMIn'. R package version **1**.

Bates, D. 2010. lme4: Mixed-effects modeling with R. Springer.

Bates, D., M. Mächler, B. Bolker, and S. Walker. 2015. Fitting linear mixed-effects models using lme4. Journal of statistical software **67**:1-48.

Burnham, K., and D. Anderson. 2002. Model Selection and Multi-model Inference. Second Edition. Springer-Verlag, New York.

Carter, A. L., M. R. Kearney, S. Hartley, W. P. Porter, and N. J. Nelson. 2018. Geostatistical interpolation can reliably extend coverage of a very high‐resolution model of temperature‐dependent sex determination. Journal of Biogeography **45**:652-663.

Gallant, J., and J. Austin. 2012a. Aspect derived from 1" SRTM DEM-S. v6. CSIRO. Data Collection. https://doi.org/10.4225/08/56D778315A62B.

Gallant, J., and J. Austin. 2012b. Slope derived from 1" SRTM DEM-S. v4. CSIRO. Data Collection. https://doi.org/10.4225/08/5689DA774564A.

Gerakis, A., and B. Baer. 1999. A computer program for soil textural classification. Soil Science Society of America Journal **63**:807-808.

Kearney, M. 2016. NicheMapR: R implementation of Niche Mapper software for biophysical modelling. R package version **1**.

Nakagawa, S., and H. Schielzeth. 2013. A general and simple method for obtaining R2 from generalized linear mixed-effects models. Methods in Ecology and Evolution **4**:133-142.

Phillips, S. J. 2008. Transferability, sample selection bias and background data in presence-only modelling: a response to Peterson et al.(2007). Ecography **31**:272-278.

Phillips, S. J., R. P. Anderson, and R. E. Schapire. 2006. Maximum entropy modeling of species geographic distributions. Ecological modelling **190**:231-259.

Phillips, S. J., and M. Dudík. 2008. Modeling of species distributions with Maxent: new extensions and a comprehensive evaluation. Ecography **31**:161-175.

R Core Team. 2021. R: A language and environment for statistical computing. R Foundation for Statistical Computing, Vienna, Austria, URL: http://www.R-project.org/.

Tomlinson, S., W. Lewandrowski, C. P. Elliott, B. P. Miller, and S. R. Turner. 2020. High‐resolution distribution modeling of a threatened short‐range endemic plant informed by edaphic factors. Ecology and evolution **10**:763-777.

Tomlinson, S., E. P. Tudor, S. R. Turner, S. Cross, F. Riviera, J. Stevens, J. Valliere, and W. Lewandrowski. 2021. Leveraging the value of conservation physiology for ecological restoration. Restoration Ecology.

Turner, N. C. 1981. Techniques and experimental approaches for the measurement of plant water status. Plant and Soil **58**:339-366.

Valliere, J. M., J. Ruscalleda Alvarez, A. T. Cross, W. Lewandrowski, F. Riviera, J. C. Stevens, S. Tomlinson, E. P. Tudor, W. S. Wong, and J. W. Yong. 2021. Restoration ecophysiology: an ecophysiological approach to improve restoration strategies and outcomes in severely disturbed landscapes. Restoration Ecology:e13571.

Viscarra Rossel, R., C. Chen, M. Grundy, R. Searle, D. Clifford, N. Odgers, K. Holmes, T. Griffin, C. Liddicoat, and D. Kidd. 2014a. Soil and Landscape Grid National Soil Attribute Maps - Clay (3" resolution) - Release 1. v5. CSIRO. Data Collection. https://doi.org/10.4225/08/546EEE35164BF.

Viscarra Rossel, R., C. Chen, M. Grundy, R. Searle, D. Clifford, N. Odgers, K. Holmes, T. Griffin, C. Liddicoat, and D. Kidd. 2014b. Soil and Landscape Grid National Soil Attribute Maps - Sand (3" resolution) - Release 1. v5. CSIRO. Data Collection. https://doi.org/10.4225/08/546F29646877E.

Viscarra Rossel, R., C. Chen, M. Grundy, R. Searle, D. Clifford, N. Odgers, K. Holmes, T. Griffin, C. Liddicoat, and D. Kidd. 2014c. Soil and Landscape Grid National Soil Attribute Maps - Silt (3" resolution) - Release 1. v5. CSIRO. Data Collection. https://doi.org/10.4225/08/546F48D6A6D48.

Appendix 1: Projected species distribution and likelihood of occurrence for *Aluta quadrata* derived from a MaxEnt model. Increasing intensity of colour (from blue to red) indicates a higher likelihood of occurrence.

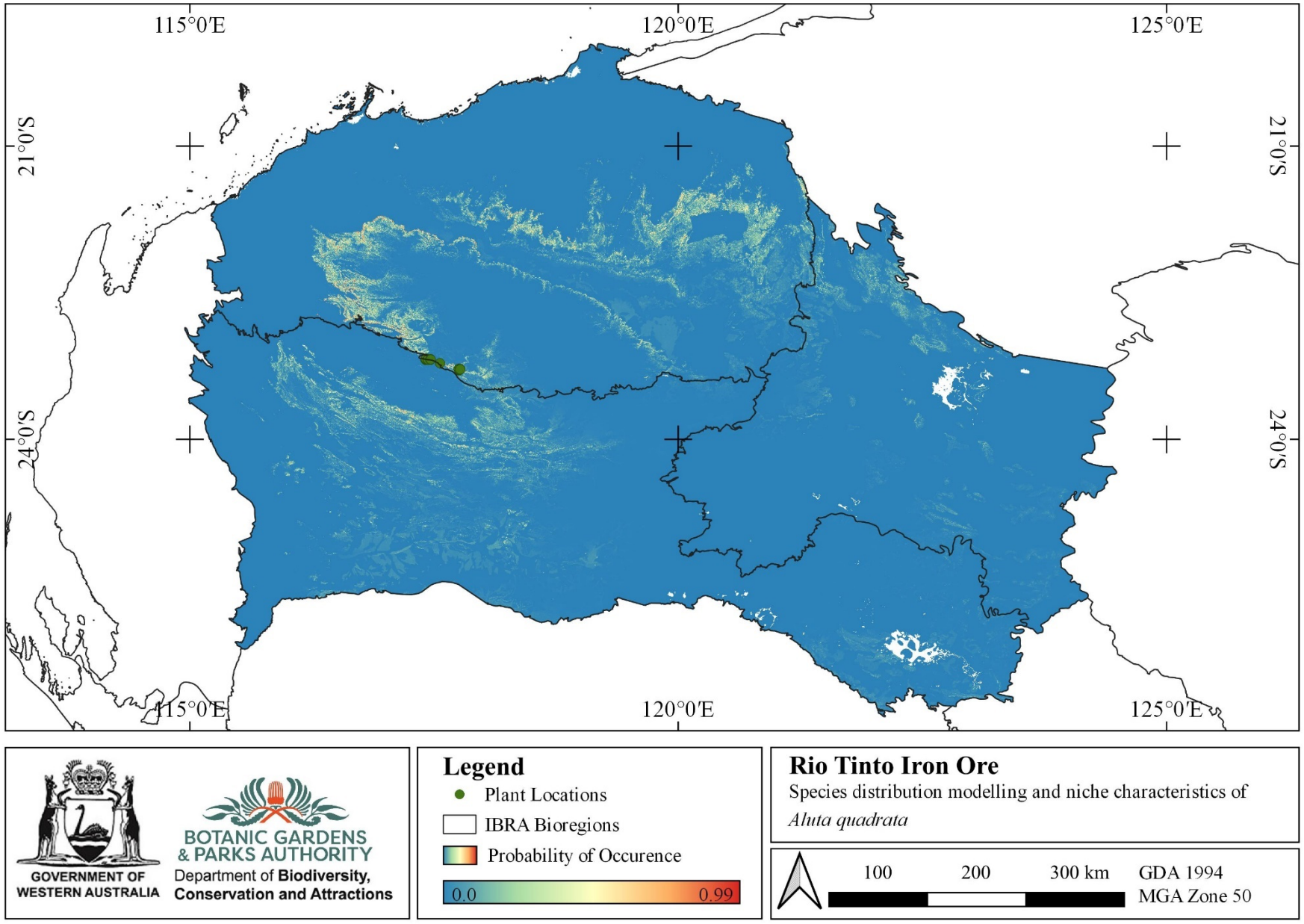

Appendix 2: Distribution extent of *Aluta quadrata* overlayed onto the projected species distribution and likelihood of occurrence derived from a MaxEnt model. Increasing intensity of colour (from blue to red) indicates a higher likelihood of occurrence.

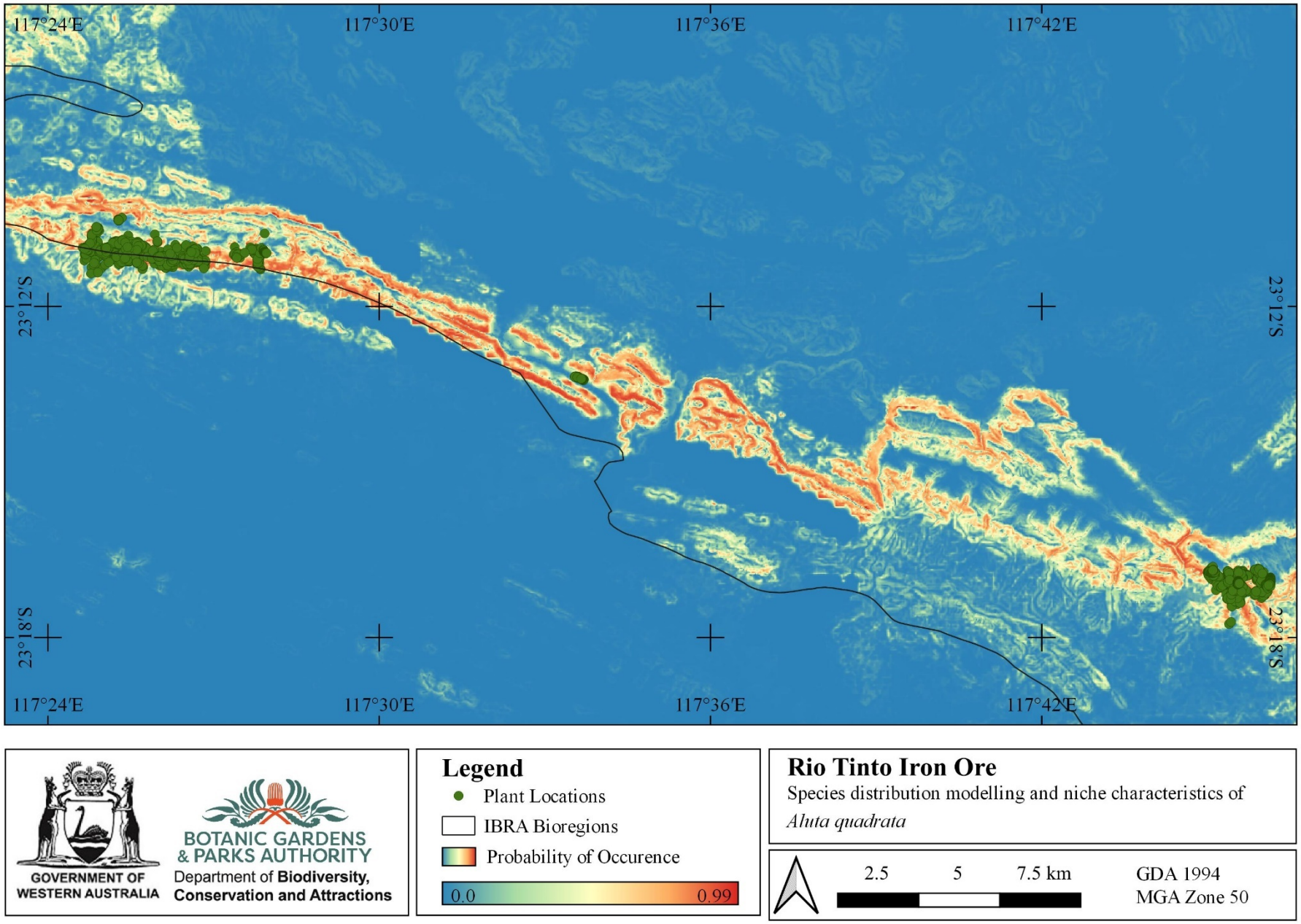

Appendix 3 : Map of the niche-model indicating the locations of the four study sites within the Western Ranges (Population 1). Results for plant functioning are presented for Sites 1 and 3 in the present report. Refer to Table 4 for the average suitability indexes for sites 1-4.

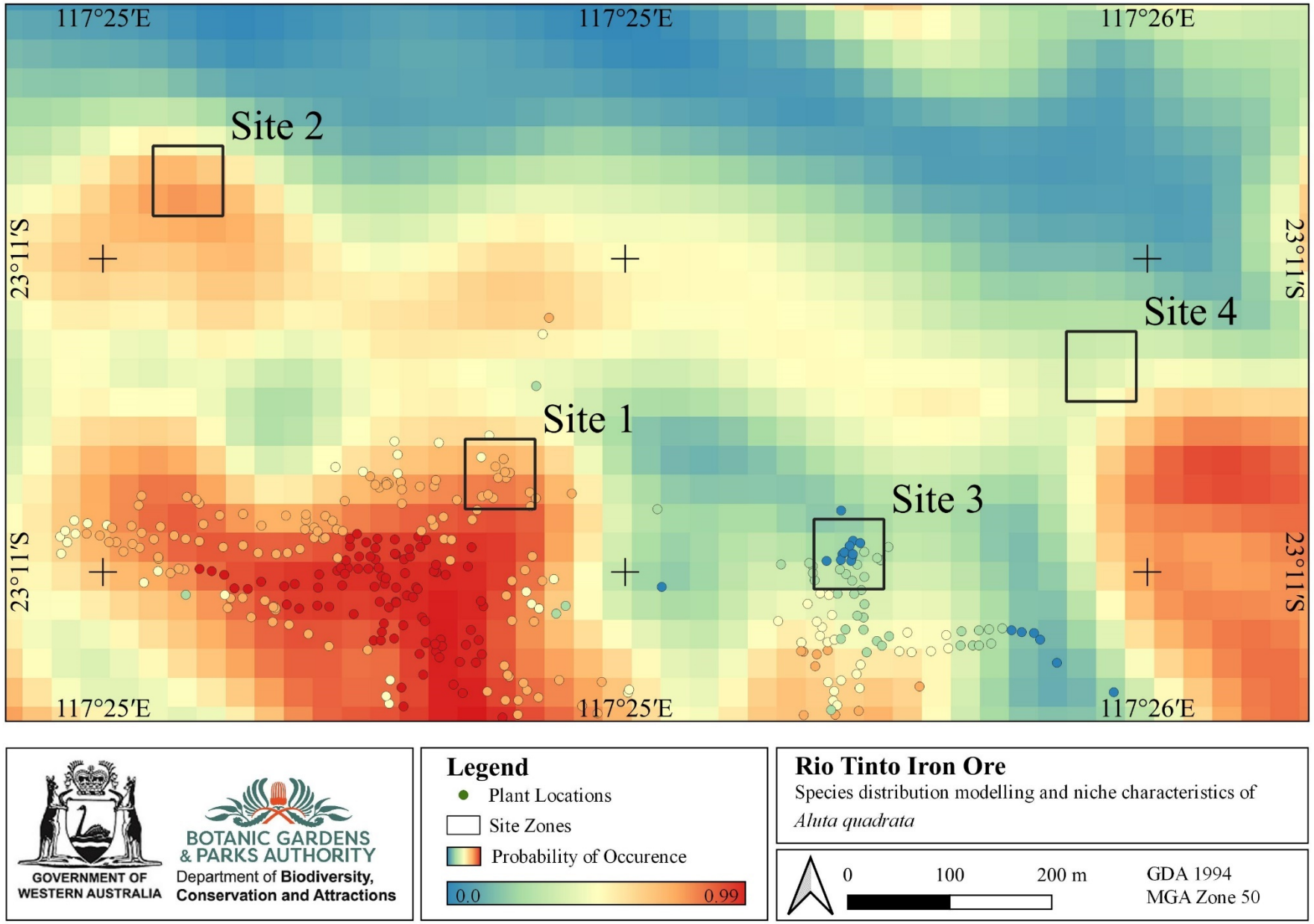

Appendix 4 : Spatial projection of slope data used to train the MaxEnt Distribution model.

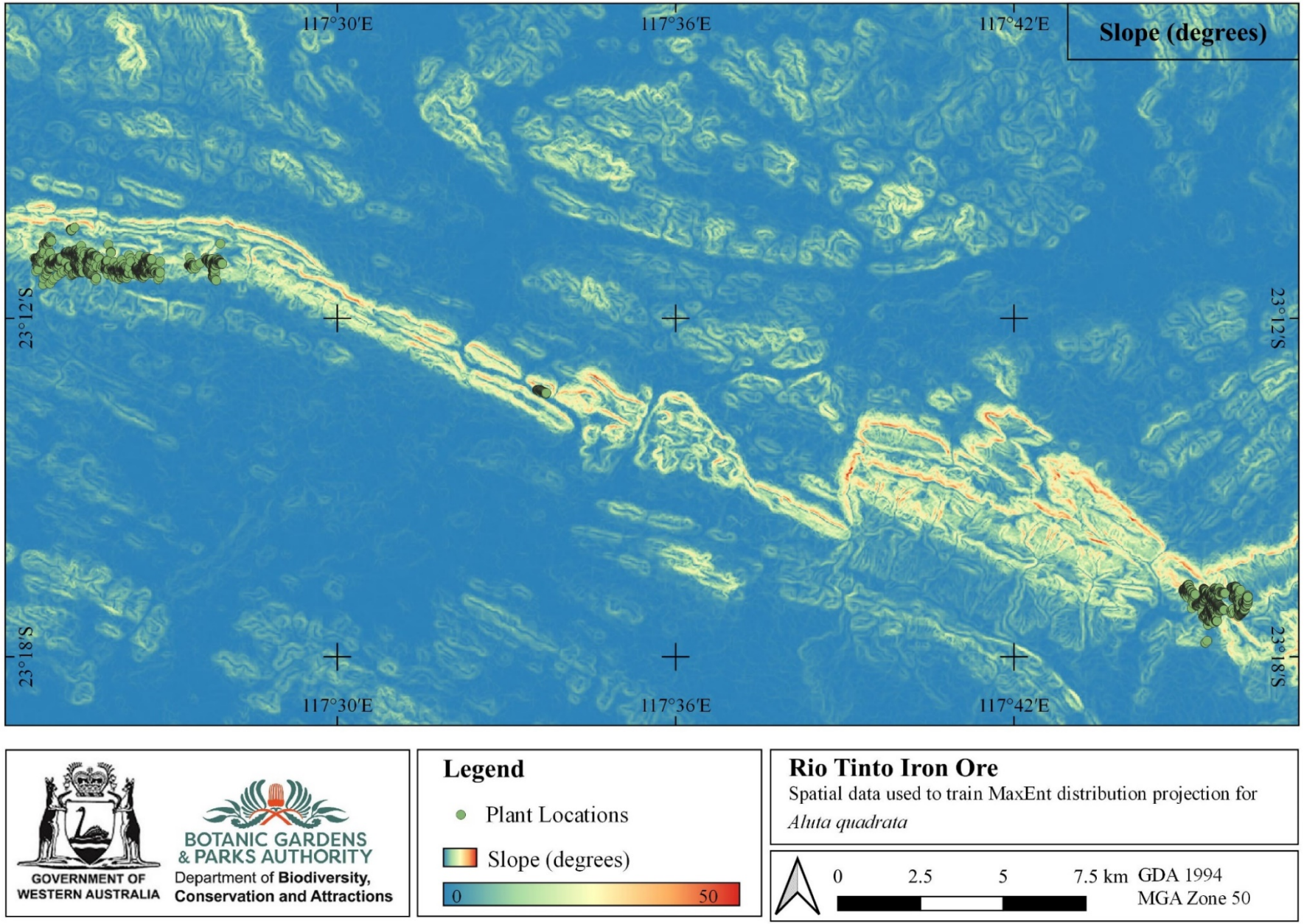

Appendix 5 : Spatial projection of elevation data used to train the MaxEnt Distribution model.

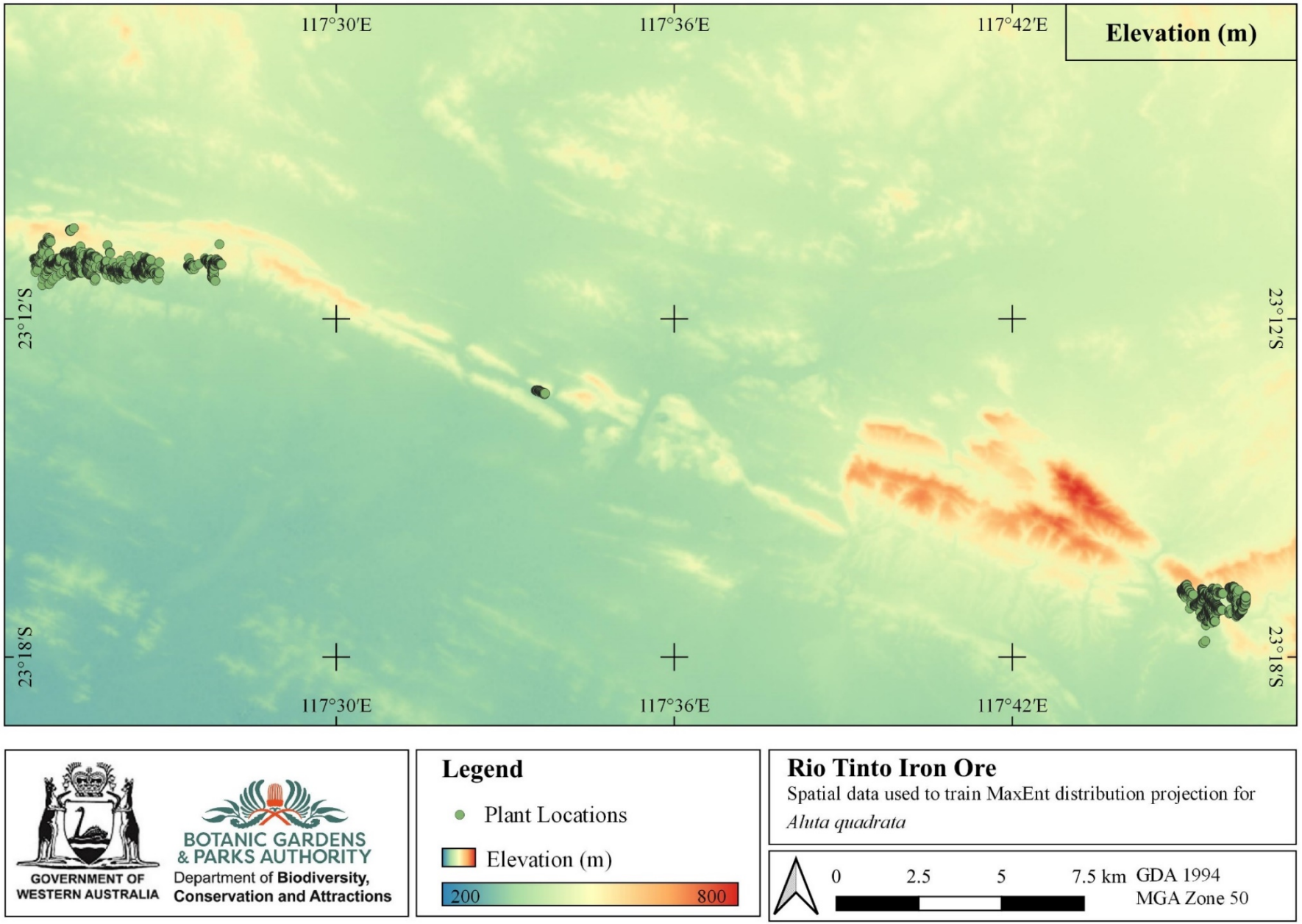

Appendix 6: Spatial projection of Slope data used to train the MaxEnt Distribution model.

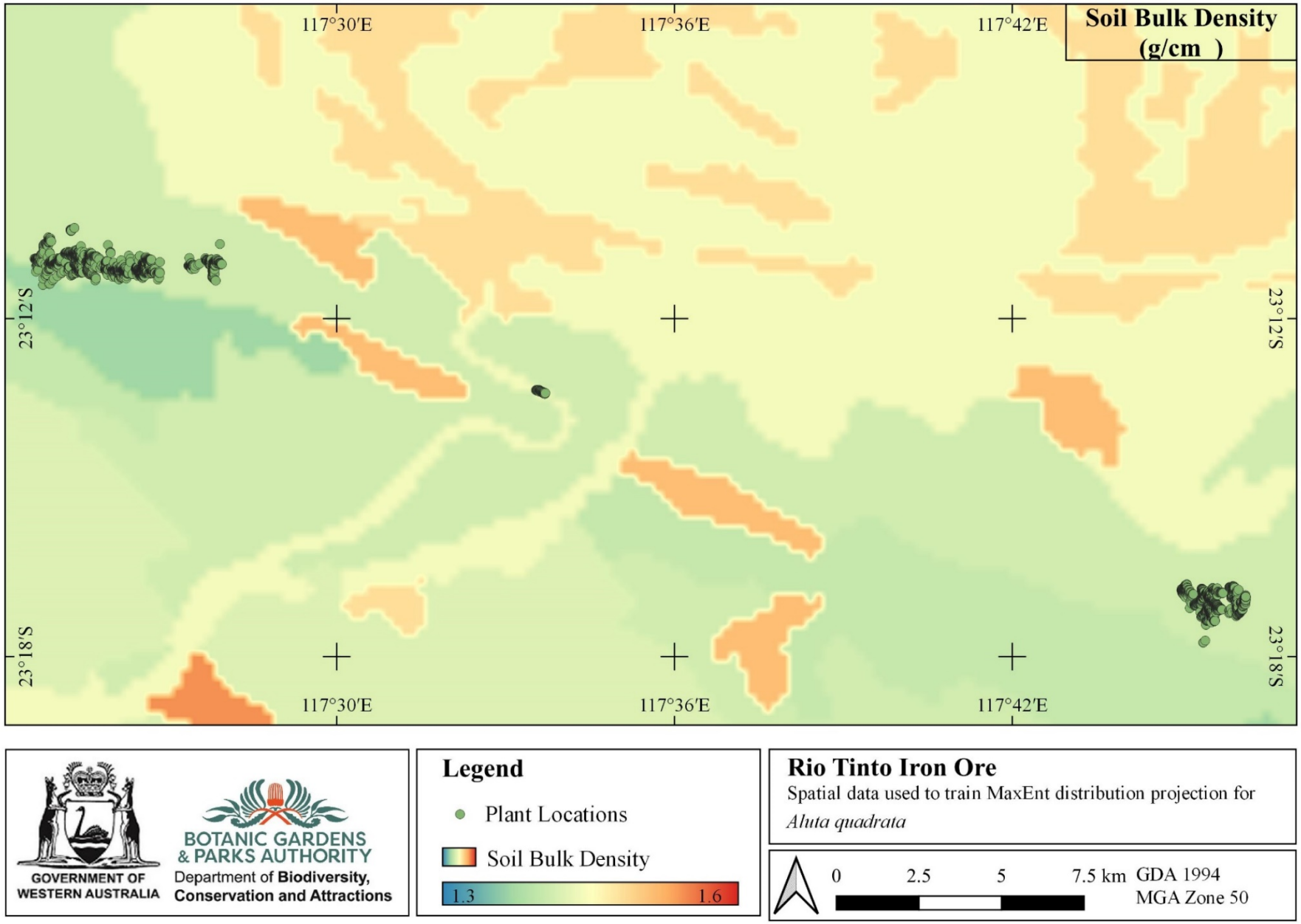

Appendix 7 : Spatial projection of Slope data used to train the MaxEnt Distribution model.

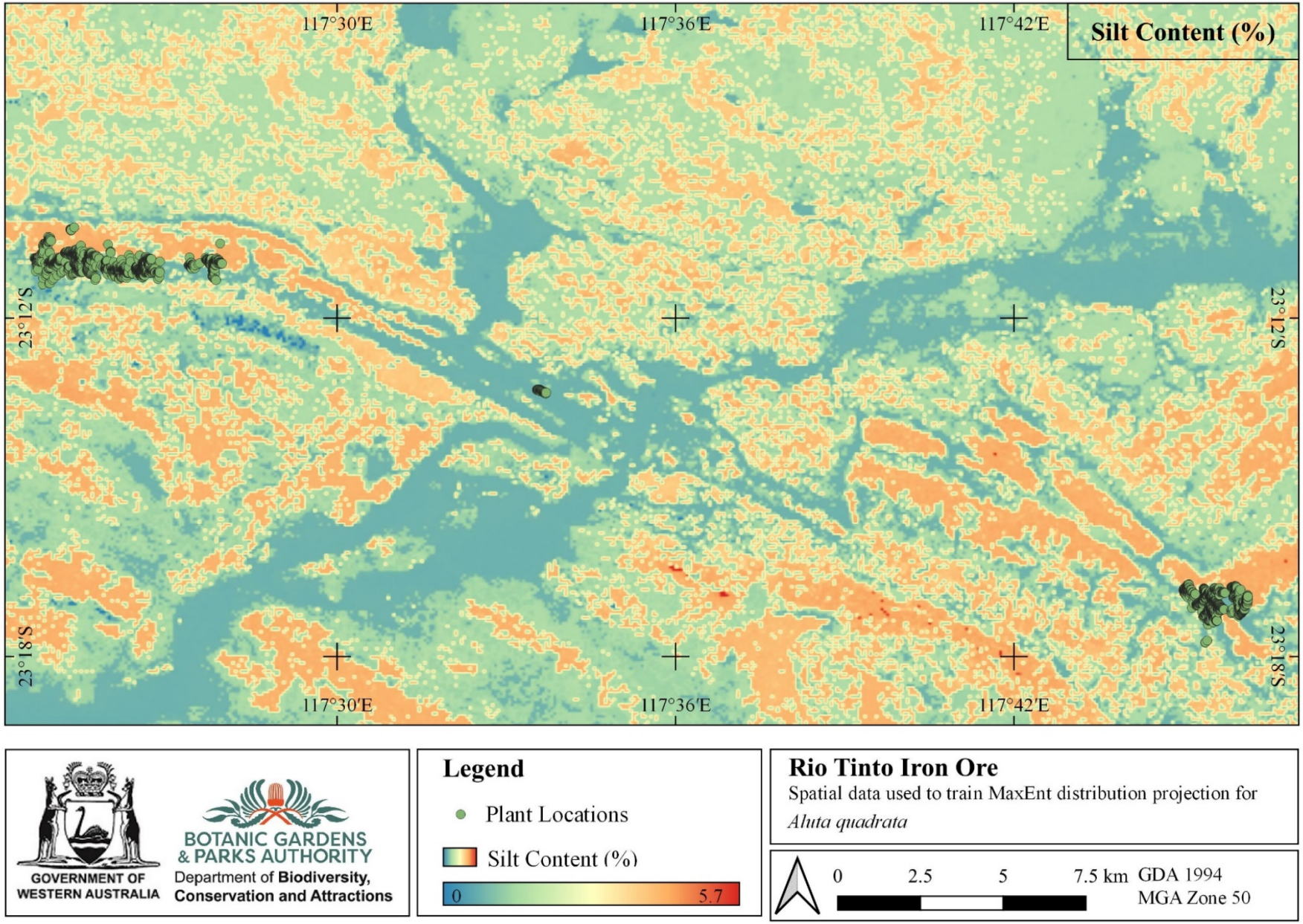

Appendix 8 : Summary statistics (mean ± se) for each edaphic variable contributing to the MaEnt Distribution model as it pertains to a categorical representation of the projected habitat suitability. Increasing intensity of colour (from blue to red) indicates a higher likelihood of occurrence and infers greater habitat suitability.

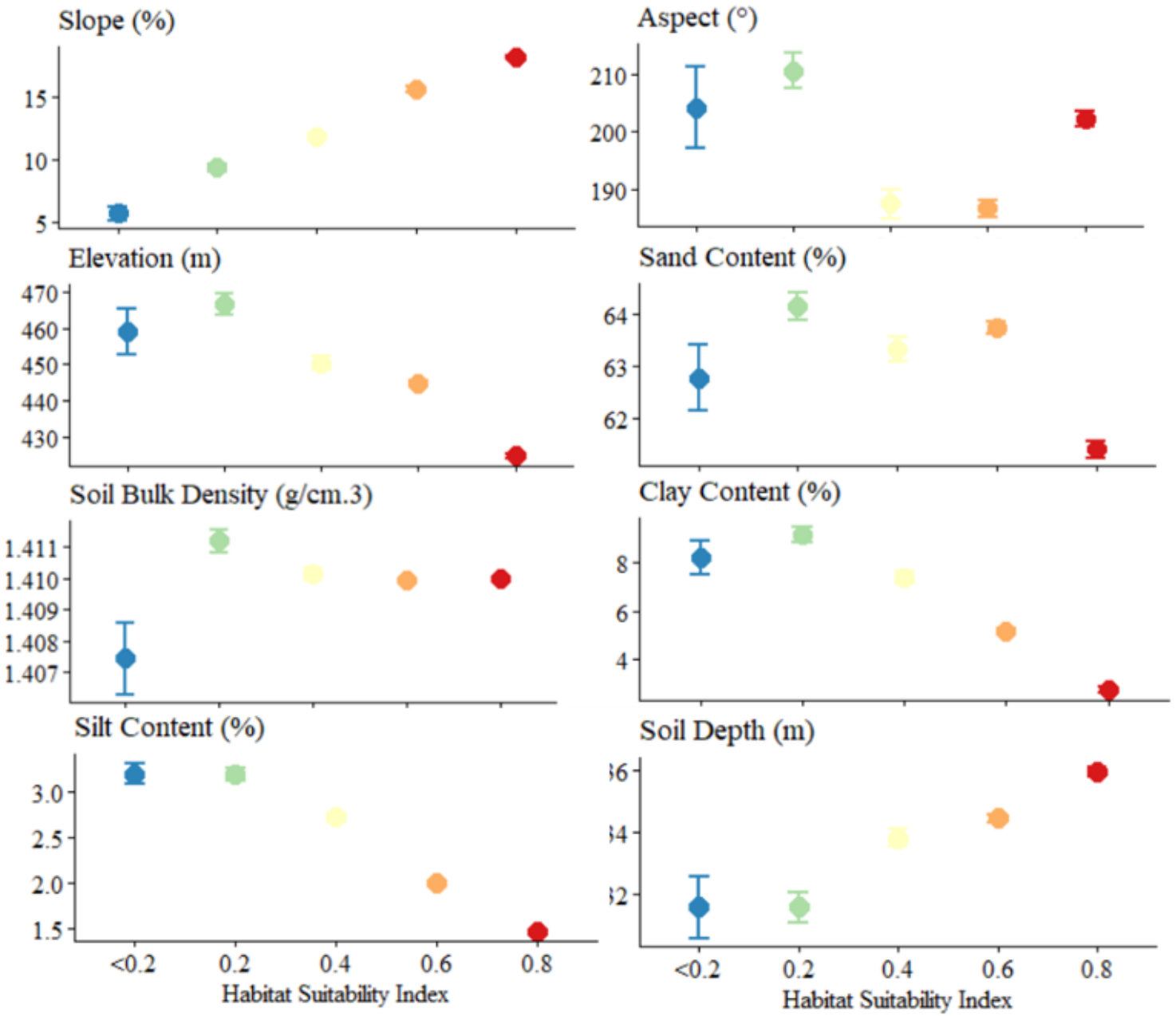

Appendix 9 : Summary statistics (mean ± se) for each microclimatic correlate associated with the MaEnt Distribution model as it pertains to a categorical representation of the projected habitat suitability. Increasing intensity of colour (from blue to red) indicates a higher likelihood of occurrence and infers greater habitat suitability.